Exploration of sequence space as the basis of viral RNA genome segmentation

Elena Moreno[a], Samuel Ojosnegros[a,1], Juan García-Arriaza[1,2], Cristina Escarmís[a], Esteban Domingo[a,b,3], and Celia Perales[a,b,3]

[a]Department of Virology and Microbiology, Centro de Biología Molecular "Severo Ochoa," Consejo Superior de Investigaciones Científicas-Universidad Autónoma de Madrid, Campus de Cantoblanco, 28049 Madrid, Spain; and [b]Centro de Investigación Biomédica en Red de Enfermedades Hepáticas y Digestivas, 08036 Barcelona, Spain

Edited by Peter Schuster, University of Vienna, Vienna, Austria, and approved March 31, 2014 (received for review December 17, 2013)

The mechanisms of viral RNA genome segmentation are unknown. On extensive passage of foot-and-mouth disease virus in baby hamster kidney-21 cells, the virus accumulated multiple point mutations and underwent a transition akin to genome segmentation. The standard single RNA genome molecule was replaced by genomes harboring internal in-frame deletions affecting the L- or capsid-coding region. These genomes were infectious and killed cells by complementation. Here we show that the point mutations in the nonstructural protein-coding region (P2, P3) that accumulated in the standard genome before segmentation increased the relative fitness of the segmented version relative to the standard genome. Fitness increase was documented by intracellular expression of virus-coded proteins and infectious progeny production by RNAs with the internal deletions placed in the sequence context of the parental and evolved genome. The complementation activity involved several viral proteins, one of them being the leader proteinase L. Thus, a history of genetic drift with accumulation of point mutations was needed to allow a major variation in the structure of a viral genome. Thus, exploration of sequence space by a viral genome (in this case an unsegmented RNA) can reach a point of the space in which a totally different genome structure (in this case, a segmented RNA) is favored over the form that performed the exploration.

RNA virus evolution | evolutionary transition | quasi-species | mutant spectrum | viral emergence

RNA viruses replicate as complex distributions of closely related genomes termed viral quasi-species (1). Quasi-species dynamics is a consequence of high mutation rates and of the intrapopulation interactions that are established among components of a mutant spectrum that can either enhance or quench the replication of the ensemble (1–7).

One extreme and unusual case of intrapopulation evolution was described with the picornavirus foot-and-mouth-disease virus (FMDV). When the biological clone FMDV C-S8c1 (8) was subjected to serial cytolytic passages in baby hamster kidney-21 (BHK-21) cells at high multiplicity of infection (MOI), the virus underwent a transition consisting in the generation of multiple genome types, each with an internal in-frame deletion (9–11) (Fig. 1 *A* and *B*). The standard genomes were at least 10^4-fold less frequent than the segmented version, termed C-S8p260. Low MOI passage of C-S8p260 rescued the standard genome (termed C-S8p260p3d), suggesting that the latter is either continuously present at very low frequency or occasionally generated. Two genomes with internal deletions dominated at passage 260: (*i*) Δ417 with a deletion that comprises part of proteinase L [genomic nucleotides 1,154–1,570 (numbering according to ref. 12)], which spans the residues encoding the catalytic amino acids (13) (Fig. 1*C*); proteinases L and 3C are involved in shut-off of host cell protein synthesis (14–16); and (*ii*) Δ999, which lacks part of VP3 and VP1 (genomic nucleotides 2,794–3,792). Δ417 and Δ999 RNAs were infectious by complementation in the absence of the standard FMDV RNA (9–11, 17). Therefore, repeated high MOI passages of a cloned FMDV resulted in a striking evolutionary transition akin to what is expected of a first step in a process of genome segmentation.

Here we address the critical question of what was the initial trigger of the transition toward segmentation. Our previous studies with the segmented FMDV version included the following: (*i*) a description of the transition toward segmentation and the complementation between the two RNA segments (10); (*ii*) measurement of fitness gain and capacity of the segmented form to interfere with replication of standard FMDV (9); (*iii*) documentation of a continuous dynamics of mutation and recombination in the course of the viral passages. Intermediate populations included multiple minority genomes with internal deletions, until Δ417 and Δ999 became dominant in C-S8p260 (11). (*iv*) A comparison of C-S8p260 and its unsegmented derivative C-S8p260p3d, which showed a 1.7-fold higher fitness for the segmented form that coincided with a 2-fold increase in specific infectivity (the ratio between the amount of infectivity and viral RNA) (17). No significant differences were found in the exponential increase of viral RNA or viral protein synthesis at early times after infection. The only significant difference detected was a higher particle stability of the segmented virus than its unsegmented counterpart (a 1.2-fold difference in

Significance

The molecular basis of a drastic evolutionary change, akin to RNA genome segmentation, previously observed with foot-and-mouth disease virus was unknown. Here we report that point mutations that accumulated in the genome during replication permitted the transition toward genome segmentation. This effect of mutations has been shown by placing the deletions in the sequence context of the parental and evolved RNAs and quantifying protein expression and infectious progeny production. The results document that an extensive exploration of sequence space was required prior to this multifactorial evolutionary transition. An unsegmented viral genome can reach a point in sequence space at which a different genomic organization is favored. The observation underlines the value of quasi-species dynamics as a factor in the emergence of viral genomes.

Author contributions: E.M., S.O., E.D., and C.P. designed research; E.M., S.O., J.G.-A., and C.P. performed research; S.O., J.G.-A., C.E., and C.P. contributed new reagents/analytic tools; E.M., S.O., J.G.-A., E.D., and C.P. analyzed data; and E.D. and C.P. wrote the paper.

The authors declare no conflict of interest.

This article is a PNAS Direct Submission.

[1]Present address: California Institute of Technology, Division of Biology, Pasadena, CA 91125.

[2]Present address: Centro Nacional de Biotecnología, Campus de Cantoblanco, 28049 Madrid, Spain.

[3]To whom correspondence may be addressed. E-mail: edomingo@cbm.uam.es or cperales@cbm.uam.es.

This article contains supporting information online at www.pnas.org/lookup/suppl/doi:10.1073/pnas.1323136111/-/DCSupplemental.

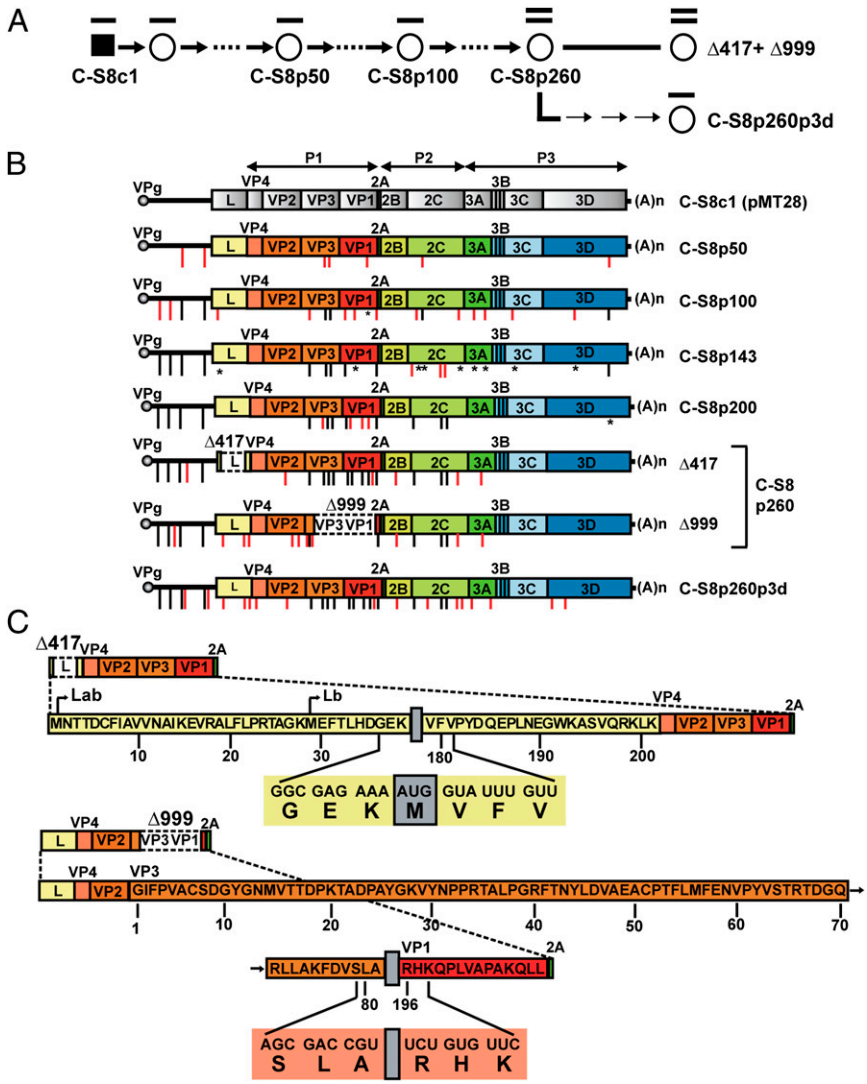

Fig. 1. Accumulation of mutations on passage of FMDV C-S8c1 in BHK-21 cells, and the transition toward genome segmentation. (*A*) Biological clone C-S8c1 (8) with the standard genome (line on filled square) was passaged in BHK-21 cells at an MOI of 2–4 PFU per cell (empty circles and thick arrows). At passage 260, the genome consisted mainly of two RNAs with internal deletions: Δ417+Δ999 (two lines on circle). Three low MOI passages of C-S8p260 (thin arrows) produced population C-S8p260p3d with the standard length genome. (*B*) Accumulation of mutations on passage of C-S8c1 (the biological clone from which pMT28 was constructed) (11). The C-S8c1 (pMT28) genome is depicted at the top, with encoded proteins represented as boxes and noncoding regions as thick lines; the P1, P2, and P3 genomic regions are denoted with lines above the genome. VPg is the 3B-coded protein, covalently linked to the 5′ end of the RNA, and (A)n is the 3′-terminal polyadenylate (27–29). Successive populations (from top to bottom) are identified on the right of each genome, with the number following p denoting the passage number. The position of each mutation is indicated by a vertical line outstanding below the corresponding genome; red lines denote mutations that appear for the first time in the lineage, and black lines are mutations that are maintained in successive passages; reversion to the residue of C-S8c1 is indicated by an asterisk. A few positions included mixed nucleotides according to the sequencing peak; a residue had to amount to more than 50% in the peak to be considered a mutation. The full list of mutations is given in Table S1. Δ417 and Δ999 are the RNAs with internal in-frame deletions within the L- and VP3, VP1-coding regions, respectively (white boxes with discontinuous lines). Procedures for infections, identification of internal deletions, and nucleotide sequencing are described in *Materials and Methods*. (*C*) Amino acid sequence of L protein in Δ417ev and of VP3-VP1 in Δ999. The breakpoint at the 5′ side of deletion Δ417 interrupts the amino acid sequence G36-E37-K38, whereas at the 3′ side, the breakpoint interrupts the sequence V179-F180-V181. The amino acid sequence that results from deletion Δ999 in the polyprotein part of the truncated capsid is SLA and RHK at the 5′ and 3′ side of the deletion, respectively, which represents elimination of amino acids 82–219 in VP3 and 1–195 in VP1. For Δ417ev, the two M residues at the N terminus of Lab and Lb are indicated. The deletion resulted in the generation of a new AUG codon, with the A originating from codon AAG at the 5′ side of the deletion and UG from codon CUG at the 3′ side of the deletion. The resulting nucleotide and amino acid sequences at the breakpoint site are depicted below the complete sequence. The Δ999 deletion did not generate any additional amino acid. The truncation sites are indicated with gray boxes. The resulting nucleotide and amino acid sequences are depicted below the complete sequence. The numbers below the sequences indicate the amino acid number of the full-length Lab and VP3-VP1 proteins of C-S8c1 (12).

inactivation rate constant) (17). This difference does not explain the initial trigger of genome segmentation, because genome segmentation and the ensuing encapsidation of two types of RNAs with deletions had to precede the selective testing of particle stability.

The initial event that led to genome segmentation is the question addressed here. We considered two possibilities: (*i*) that the location of the deletions, irrespective of the nucleotide sequence context, conferred the selective advantage to the segmented form, or (*ii*) that the transition toward segmentation and

efficient complementation required accompanying mutations in the evolving quasi-species and that only when such mutations were present did the genomes with deletions acquire a selective replicative advantage over the standard genome.

FMDV mRNA is translated into a polyprotein that is cleaved to produce a number of functional processing intermediates and mature proteins (18). We compared protein expression, progeny production, and complementation activity of the two genomes with internal deletions in the sequence context of P2, P3 (nonstructural protein-coding region) of the evolved C-S8p260 genomes and in the sequence context of pMT28 [a molecular clone derived from C-S8c1 (10) used for the constructions described in the present study]. The results indicate a key contribution of point mutations generated in the course of FMDV replication in allowing the segmented genome to acquire a selective advantage over its matching standard genome. Complementation between the two ΔRNAs is multifactorial, and the leader proteinase L plays a pivotal role in the complementation activity. It is known that explorations in sequence space promote virus adaptability. In the case of FMDV, the results show that exploration of sequenced space by the standard FMDV through point mutations led the virus to a point in which the highest positive impact for fitness was not for the genome that performed the exploration but for a totally different segmented form. We discuss the importance of movements in sequence space through mutation to promote genome segmentation in an RNA virus and generally for large evolutionary transition in viruses.

Results

Dependence of the Selective Advantage of Genomes with Internal Deletions on the Sequence Context. The segmented FMDV genome at passage 260 (C-S8p260) differed from the parental virus C-S8c1 (pMT28) in 30 mutations (Fig. 1 and Table S1). To investigate a possible influence of acquired mutations in the fitness of the segmented genome version, the deletions were introduced in the FMDV genome in the context of the nonstructural protein-coding region (P2, P3; residues 4,201–7,427) of either the parental (pa) virus C-S8c1 (pMT28), or the evolved (ev) C-S8p260p3d genome; this genome is derived from C-S8p260 by three low MOI passages, and its P2, P3 region includes the same nonsynonymous mutations that were dominant in C-S8p260 (Fig. 1 and Tables S1 and S2). The two forms are termed Δ417pa or Δ999pa when the sequence context of the nonstructural protein-coding region is that of pMT28 and Δ417ev or Δ999ev when the context is that of C-S8p260p3d (Fig. 2*A*). To compare viral and host protein expression, the engineered and control RNAs were electroporated individually into BHK-21 cells, and proteins were pulse-labeled at different hours after electroporation (HPE) and analyzed electrophoretically and by Western blot (Fig. 2 *B* and *C*). Shutoff of host protein synthesis that accompanies aphthovirus infections is reflected in the cellular protein patterns (Fig. 2*B*). The increase in viral protein expression level mediated by the point mutations was 165-fold for the ΔRNAs and only 3.3-fold for the standard unsegmented RNA ($P < 0.001$; ANOVA test; average values for each expressed viral protein according to the Western blots shown in Fig. 2*C*, with normalization to the amount of actin). Thus, the accumulation of point mutations had a 50-fold higher positive effect in protein expression from the segmented FMDV genome than from the corresponding unsegmented counterpart. Active protein expression from the RNAs harboring internal deletions occurred when the latter was located within the P2, P3 context of the evolved FMDV genome but not of the parental genome.

Effect of Point Mutations on Gene Expression and Infectious Progeny Production of Segmented FMDV. To investigate whether a specific amino acid substitution was responsible for the enhanced replicative capacity of Δ417ev and Δ999ev RNAs, the five nonsynonymous mutations present in the 2C- and 3A-coding region of Δ417ev and Δ999ev (Table S2) were introduced individually in the sequence context of Δ417pa and Δ999pa and protein expression analyzed. Infectious progeny was produced following coelectroporation with Δ417ev + Δ999ev RNAs (with the entire constellation of mutations in P2, P3 present), but not with Δ417pa + Δ999pa RNAs (that is, devoid of mutations) ($P = 0.01$; ANOVA test). Infectivity was rescued when the parental RNAs expressed 2C with either T256A or Q263H, or 3A with D103G (Fig. S1). Thus, no single amino acid substitution within 2C or 3A accounted for the fitness increase of the evolved version of the segmented genome. Substitutions T256A and Q263H in 2C that were dominant in passage 200, before the segmented form became dominant, had a minor but positive effect on Δ417pa + Δ999pa protein expression and progeny production, suggesting a gradual exploration of sequence space that approximated the system toward segmentation. The extent of shutoff of host cell protein synthesis was commensurate with the level of viral protein expression (Fig. S2). ΔRNAs, with no standard FMDV RNA, were detected in the cell culture supernatants using specific RT-PCR amplifications (Fig. S3). Therefore, the constellation of point mutations in the P2, P3 region permitted the segmented FMDV version to produce infectious progeny.

Molecular Basis of Complementation Between ΔRNAs. Because the only region lacking in Δ417ev RNA is that encoding the leader proteinase L, we hypothesized that supply of L *in trans* might compensate for the absence of Δ999ev RNA. To test this possibility, FMDV L and poliovirus (PV) protein 2A (a viral protease as negative control for FMDV processing events) were expressed *in trans*. L and 2A were functional because they cleaved translation factor eIF4GI (Fig. S4). Although PV 2A did not alter the proteins expressed from Δ417ev RNA (including the predicted chimeric precursors Δ417-VP0), FMDV L cleaved such precursors yielding VP0 (Fig. 3 and Fig. S4). A *trans*-expression of L resulted in a 14-fold increase of infectious Δ417ev RNA ($P < 0.01$; ANOVA test), indicating a key role of this protein in the complementation between ΔRNAs (Fig. 3) (L affected the pattern of protein processing from Δ417ev RNA, and these results will be described elsewhere).

In conclusion, a major evolutionary transition toward segmentation of a picornaviral genome necessitated extensive exploration of sequence space during extended replication to attain a constellation of point mutations that conferred a selective advantage to the bipartite FMDV genome. Despite the actor of the exploration being the standard unsegmented genome, the product of exploration was a point of sequence space at which a drastically different, segmented genomic form was favored over the unsegmented form that performed the exploration.

Discussion

We documented that an unusual evolutionary transition that converted the unsegmented positive strand FMDV RNA into complementing genomes harboring internal deletions was made possible by point mutations that accumulated in the viral genome (Figs. 1 and 2, Fig. S1, and Tables S1 and S2). Active viral polyprotein expression and processing, as well as infectious progeny production, were observed when the internal deletions were placed under the sequence context of the nonstructural protein-coding region (P2, P3) of the evolved FMDV C-S8p260p3d but not of the parental FMDV pMT28. These results imply that if the same deletions had occurred at the early evolutionary phases of C-S8c1, the segmented version would have been outcompeted by the standard genome. In fact, such a major transition has never been observed in other passage experiments of persistent or cytopathic FMDV in cell culture (19). The required context of point mutations was

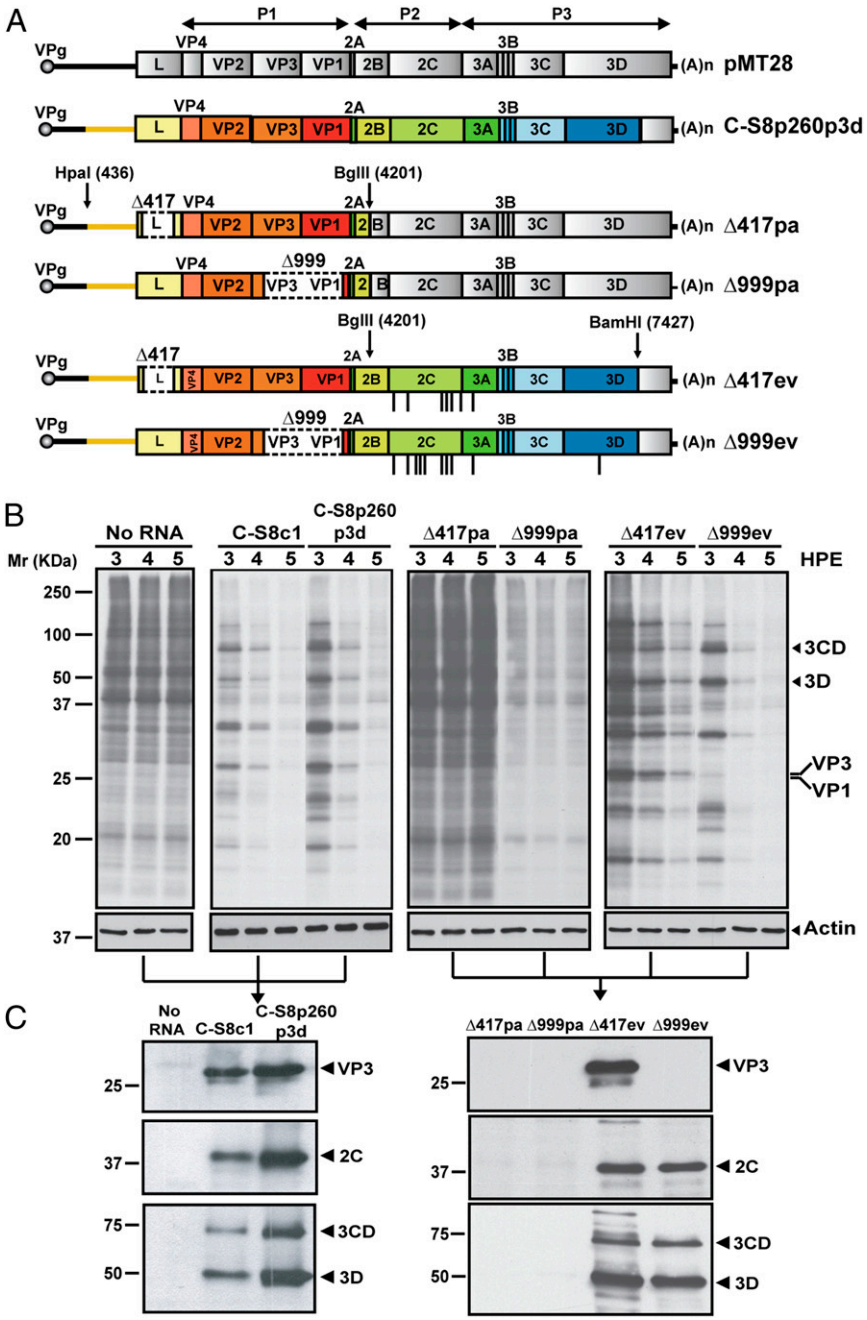

Fig. 2. Scheme of parental and chimeric FMDV genomes and patterns of protein expression. (*A*) Genomes are represented with coding and noncoding regions with symbols and nomenclature as in Fig. 1. Δ417pa and Δ999pa depict the constructs in which the in-frame deletions in the L- and VP3, VP1-coding regions (white boxes with discontinuous lines) were placed under the sequence context of the nonstructural protein region of the parental C-S8c1 (in gray). Δ417ev and Δ999ev describe the constructs in which the same deletions were placed under the sequence context of the nonstructural protein region of the evolved C-S8p260 (in color). Vertical lines outstanding below the corresponding genome indicate the mutations that distinguish Δ417ev and Δ999ev from Δ417pa and Δ999pa (Tables S1 and S2). The sequences of the nonstructural protein-coding region are those of two molecular clones isolated from population C-S8p260p3d. (*B*) The indicated FMDV RNAs (25 μg) transcribed from the DNAs depicted in *A* and identified above the corresponding lanes were electroporated into BHK-21 cells. No RNA lanes mean mock-electroporated cells. Then the electroporated cells were labeled with [^{35}S] Met-Cys for 1 h (2–3, 3–4, and 4–5 h after electroporation, abbreviated as 3, 4, and 5 HPE, respectively, in the different lanes), and the cell extracts were analyzed by SDS/PAGE, followed by fluorography and autoradiography. The pattern of viral proteins as a function of time PE is expected from genomes with deletions in the L-coding region (Δ417) and in the capsid-coding region (Δ999). The position of 3CD, 3D, VP3, and VP1 is indicated. The amount of extract analyzed was normalized using actin (bottom bands). (*C*) Western blot analysis of FMDV proteins from the lanes at 4 HPE from *B*. Proteins were identified by their reactivity with monoclonal antibodies specific for VP3 and 2C, and a polyclonal antibody against 3D, that have been previously described (30, 31). Note that VP3 is absent among the expression products of Δ999ev because the RNA lacks most of the VP3- and VP1-coding regions (compare with *A*). In *B* and *C*, the numbers on the left indicate molecular mass markers (M_r, kDa) for proteins. Procedures are detailed in *Materials and Methods*.

attained as a result of a prolonged exploration of sequence space provided by infections carried out at high MOI with sustained infecting FMDV populations above 10^7 PFU. The ensemble of accumulated mutations may contribute to the adequate phenotype at the RNA or protein level or both. The results suggest that RNA genomes harbor potential for drastic

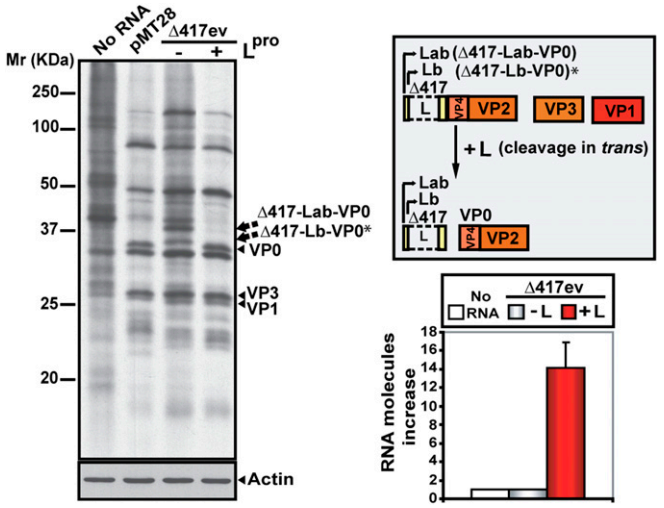

Fig. 3. Role of proteinase L in the complementation between ΔRNAs. (*A*) Electropherogram of proteins expressed on electroporation of BHK-21 cells with 25 μg of Δ417ev RNA, in the absence or presence of L expressed from plasmid pTM1-L (30 μg) at 4 HPE. No RNA means mock-electroporated cells, and pMT28 means expression from pMT28 RNA used as control. The positions of some viral proteins and protein precursors are indicated on the right. The predicted proteolytic cleavages of proteins on coelectroporation of L protein in *trans* are indicated in the top right box. The asterisk next to Δ417-Lb-VP0 indicates that this product could originate at any of the two methionines (M29 or M39) encoded by Δ417ev. As controls, Δ417Lab-VP0 and Δ417Lb-VP0 were not processed by poliovirus protein 2A, whereas both FMDV L and poliovirus 2A cleaved eIF4G-I (Fig. S4). The supernatant obtained from the electroporated cells was used to infect a new cell BHK-21 monolayer. After 1 h of adsorption, cells were washed, and intracelullar RNA was measured by quantitative RT-PCR with specific primers (Table S3). The fold increase due to L expression is displayed at the bottom right box.

evolutionary transitions conditional on reaching combinations of point mutations.

The proteins encoded by the P2- and P3-coding regions were not expected to differ when they were expressed either from Δ417ev RNA or Δ999ev RNA because the deletions in the ΔRNAs affect only the P1-coding region. This prediction was largely confirmed by the analyses of protein expression with the unexpected observation that L also had some effect in the expression of P2, P3. The supply of L *in trans* by Δ999ev is a key determinant of the complementation activity between the ΔRNAs.

Interestingly, alternation of long quasi-stationary epochs characterized by movements in the neutral sequence space and short adaptive phases have been observed in theoretical models of evolutionary optimization (20–22). In these models, molecules evolve through mutation to attain a secondary structure that defines the target phenotype, and mutations create the adequate sequence to initiate an adaptive phase. The movement in sequence space of FMDV in our experimental system results in fitness gain, as expected from continuous replication and viral quasi-species optimization. This movement did not alter the genome organization that remained unsegmented for an extended period of replication. Interestingly, in such movement, a point was reached at which the accumulated mutations rendered the virus more fit to be segmented than unsegmented, thus interrupting a long phase of structural invariance. Regarding virus evolution and the origin of new viral pathogens, our results document the importance of exploration of sequence space by viral quasi-species, not only to gain an adaptive advantage in front of environmental demands, but, most importantly, to reach points at which a drastically different genome organization can be not only tolerated but favored. The results bring about the interesting possibility for virus evolution that mutational changes and drastic genomic alterations might be linked processes.

Materials and Methods

Cells and Virus. The origin of FMDV pMT28 and procedures for infection of BHK-21 cells have been described (8, 23, 24). FMDV C-S8p260 is a viral population obtained after 260 serial cytolytic passages of C-S8c1 [the biological clone from which molecular clone pMT28 was derived (10)] at high MOI in BHK-21 cells (2–4 PFU per cell; for each passage, 2×10^6 BHK-21 cells were infected with the virus contained in 200 μL of the supernatant from the previous infection, that included $2 \times 10^7 - 4 \times 10^7$ PFU) (9–11, 17). FMDV C-S8p260p3d is a viral population obtained after three serial cytolytic passages of C-S8p260 at a MOI of 10^{-3} PFU per cell (2×10^6 BHK-21 cells infected with 200 μL of a 10^{-3} dilution of the supernatant from the previous infection), as previously described (9–11, 17). The P2, P3-coding region of C-S8p260p3d includes the same nonsynonymous substitutions that were dominant in C-S8p260, in addition to transition A5713G (amino acid substitution N139D), which was present at a frequency of 50% in both Δ417ev and Δ999ev populations. The GenBank accession numbers for the viral genomes used in the present study are as follows: AJ133357 (C-S8c1); DQ409183 (Δ417ev); DQ409184 (Δ999ev), and DQ409185 (C-S8p260p3d).

Construction of Molecular Clones Encoding FMDV-Defective Genomes. The segmented virus version with the nonstructural protein coding region (P2, P3) of C-S8c1 was constructed using pMT28 to yield the virus made of two segments, as previously described (10). The plasmids that yield this segmented virus are termed Δ417pa and Δ999pa, and the transcribed RNAs are termed Δ417pa RNA and Δ999pa RNA. To obtain the segmented virus with the deletions in the context of the nonstructural protein-coding region (P2, P3) of the evolved C-S8p260, the nonstructural protein-coding region of C-S8p260p3d was amplified by RT-PCR with the primer pairs 2BR1-3CD1 and 3AR3-AV2new (Table S3), and AMV-RT (Promega) and Pfu polymerase (Stratagene). The two amplicons were shuffled using 2BR1 and AV2new as external primers. The DNA products were purified by low melting agarose (Cambrex) gel electrophoresis, and the DNA was purified using the Wizard PCR Preps DNA Purification System (Promega) and quantified by Sybr Safe staining in analytical gel electrophoresis with known amounts of DNA markers. The DNA was digested with BglII (genomic position 4,201) and BamHI (position 7,427). The DNA fragments were purified and ligated to plasmids Δ417pa and Δ999pa, previously digested with the same enzymes, using T4 DNA ligase (Roche). The resulting plasmids are termed Δ417ev and Δ999ev and give rise to transcripts Δ417ev RNA and Δ999ev RNA. A plasmid encoding the full-length RNA of C-S8p260p3d was constructed by introducing the L-coding region of Δ999ev [excised with a restriction fragment from position 638 (XbaI) to position 2,046 (XbaI)] into Δ417ev (treated with the same enzymes), using T4 DNA ligase. The procedures for DNA characterization and purification were as described for the construction of Δ417ev and Δ999ev. Therefore, the segmented FMDV version encoding Δ417pa, Δ999pa and the one encoding Δ417ev, Δ999ev differ only in the sequence context of the P2, P3-coding region; the sequence of P1 is identical in the two viruses.

Δ417pa and Δ999pa were used as the genomic backbone for the construction of the five mutant infectious clones: S80N, T256A, Q263H, and M283V in 2C and D103G in 3A. An RT-PCR product from C-S8c1 RNA, using 2BR3 and 3CD1 primers, was cloned into pGEM-T (Promega). Site-directed mutagenesis was performed using the corresponding primers (Table S2), and the correct clones for the five mutants were sequenced to confirm that no unwanted mutations had been introduced. The DNA was digested with BglII and RsrII, and mutant genome fragments were subsequently ligated with the similarly digested Δ417pa and Δ999pa to construct DNA clones of each mutant.

Expression of FMDV L. Plasmid pTM1-L was obtained with primers 5′NcoI-L and 3′BamHI-L, which were designed for PCR amplification of the Lab-coding region from pMT28. The resulting DNA fragment was digested with NcoI and BamHI and ligated to plasmid pTM1 containing the 5′ UTR of the encephalomyocarditis virus (kindly provided by L. Carrasco, Centro de Biología Molecular "Severo Ochoa," Universidad Autónoma de Madrid, Cantoblanco, Madrid). Plasmid pTM1-2A containing the poliovirus 2A sequence was obtained as previously described (25). The in vitro transcription and polyadenylation were performed with T7 polymerase (Promega) and poly (A) polymerase (Gibco), respectively, as specified by the manufacturers.

RNA Quantification, RT-PCR Amplification, Transcription, and Electroporation of BHK-21 Cells. Viral RNA quantification with the Light Cycler instrument (Roche), RT-PCR amplification using AMV reverse transcriptase (Promega) and Expand High Fidelity (Roche), in vitro transcription, and electroporation of BHK-21 cells have been previously described (10, 26).

Protein Analysis, Fluorography, and Western Blot Analysis. Proteins were labeled by the addition of 60 μCi of [^{35}S] Met-Cys (Amersham) per milliliter contained in Met-free DMEM, at the time postelectroporation indicated for each assay. After 1 h of incubation of the cell monolayers with the radioactive medium, the medium was removed, and the cells were harvested in 0.1 mL of sample buffer (160 mM Tris·HCl, pH 6.8, 2% (wt/vol) SDS, 11% (wt/vol) glycerol, 0.1 M DTT, and 0.033% bromophenol blue). The samples were boiled for 5 min, and aliquots were analyzed by SDS/PAGE at 200 V and subjected to fluorography and autoradiography (Table S4). The amount of extract analyzed was normalized using actin, identified with a specific mAb (anti–β-actin clone AC-15; Sigma). The amount of extract analyzed corresponded to the linear region of the relationship between the amount of extract and the intensity of the actin band by Western blot. Procedures for Western blot analyses have been previously described (26).

ACKNOWLEDGMENTS. We thank N. Sevilla (Centro de Investigación en Sanidad Animal, Instituto Nacional de Investigaciones Agrarias) for help with some experiments, I. Ventoso and L. Carrasco for the supply of the plasmid pTM1-2A expressing poliovirus protein 2A, L. Ortíz for contribution to the initial experiments of this study, M. A. Martín-Acebes for help with statistics, and A. I. De Ávila and M. E. Soria for expert technical assistance. This work was supported by Ministerio de Ciencia e Innovación (Grant BFU 2011-23604) and Fundación Ramon Areces. Centro de Investigación Biomédica en Red de Enfermedades Hepáticas y Digestivas is funded by the Instituto de Salud Carlos III. S.O. was supported by a fellowship from Ministerio de Educación y Ciencia, and J.G.-A. was supported by a fellowship from Ministerio de Sanidad y Consumo.

1. Domingo E, Sheldon J, Perales C (2012) Viral quasispecies evolution. *Microbiol Mol Biol Rev* 76(2):159–216.
2. Eigen M, Schuster P (1979) *The Hypercycle. A Principle of Natural Self-Organization* (Springer, Berlin).
3. Eigen M, McCaskill J, Schuster P (1988) Molecular quasi-species. *J Phys Chem* 92(24): 6881–6891.
4. Biebricher CK, Eigen M (2006) What is a quasispecies? *Curr Top Microbiol Immunol* 299:1–31.
5. Shirogane Y, Watanabe S, Yanagi Y (2012) Cooperation between different RNA virus genomes produces a new phenotype. *Nat Commun* 3:1235.
6. Crowder S, Kirkegaard K (2005) Trans-dominant inhibition of RNA viral replication can slow growth of drug-resistant viruses. *Nat Genet* 37(7):701–709.
7. Lauring AS, Andino R (2010) Quasispecies theory and the behavior of RNA viruses. *PLoS Pathog* 6(7):e1001005.
8. Sobrino F, Dávila M, Ortín J, Domingo E (1983) Multiple genetic variants arise in the course of replication of foot-and-mouth disease virus in cell culture. *Virology* 128(2): 310–318.
9. García-Arriaza J, Domingo E, Escarmís C (2005) A segmented form of foot-and-mouth disease virus interferes with standard virus: A link between interference and competitive fitness. *Virology* 335(2):155–164.
10. García-Arriaza J, Manrubia SC, Toja M, Domingo E, Escarmís C (2004) Evolutionary transition toward defective RNAs that are infectious by complementation. *J Virol* 78(21):11678–11685.
11. García-Arriaza J, Ojosnegros S, Dávila M, Domingo E, Escarmís C (2006) Dynamics of mutation and recombination in a replicating population of complementing, defective viral genomes. *J Mol Biol* 360(3):558–572.
12. Escarmís C, Dávila M, Domingo E (1999) Multiple molecular pathways for fitness recovery of an RNA virus debilitated by operation of Muller's ratchet. *J Mol Biol* 285(2): 495–505.
13. Guarné A, et al. (1998) Structure of the foot-and-mouth disease virus leader protease: A papain-like fold adapted for self-processing and eIF4G recognition. *EMBO J* 17(24): 7469–7479.
14. Belsham GJ, McInerney GM, Ross-Smith N (2000) Foot-and-mouth disease virus 3C protease induces cleavage of translation initiation factors eIF4A and eIF4G within infected cells. *J Virol* 74(1):272–280.
15. Lamphear BJ, Kirchweger R, Skern T, Rhoads RE (1995) Mapping of functional domains in eukaryotic protein synthesis initiation factor 4G (eIF4G) with picornaviral proteases. Implications for cap-dependent and cap-independent translational initiation. *J Biol Chem* 270(37):21975–21983.
16. Devaney MA, Vakharia VN, Lloyd RE, Ehrenfeld E, Grubman MJ (1988) Leader protein of foot-and-mouth disease virus is required for cleavage of the p220 component of the cap-binding protein complex. *J Virol* 62(11):4407–4409.
17. Ojosnegros S, et al. (2011) Viral genome segmentation can result from a trade-off between genetic content and particle stability. *PLoS Genet* 7(3):e1001344.
18. Martínez-Salas E, Ryan MD (2010) Translation and protein processing. *The Picornaviruses*, eds Ehrenfeld E, Domingo E, Roos RP (ASM Press, Washington, DC), pp 141–164.
19. Domingo E, et al. (2003) Evolution of foot-and-mouth disease virus. *Virus Res* 91(1): 47–63.
20. Fontana W, Schuster P (1998) Continuity in evolution: On the nature of transitions. *Science* 280(5368):1451–1455.
21. Schultes EA, Bartel DP (2000) One sequence, two ribozymes: Implications for the emergence of new ribozyme folds. *Science* 289(5478):448–452.
22. Schuster P, Fontana W, Stadler PF, Hofacker IL (1994) From sequences to shapes and back: A case study in RNA secondary structures. *Proc Biol Sci* 255(1344):279–284.
23. Domingo E, Dávila M, Ortín J (1980) Nucleotide sequence heterogeneity of the RNA from a natural population of foot-and-mouth-disease virus. *Gene* 11(3-4):333–346.
24. Toja M, Escarmís C, Domingo E (1999) Genomic nucleotide sequence of a foot-and-mouth disease virus clone and its persistent derivatives. Implications for the evolution of viral quasispecies during a persistent infection. *Virus Res* 64(2):161–171.
25. Ventoso I, Carrasco L (1995) A poliovirus 2A(pro) mutant unable to cleave 3CD shows inefficient viral protein synthesis and transactivation defects. *J Virol* 69(10): 6280–6288.
26. Perales C, Mateo R, Mateu MG, Domingo E (2007) Insights into RNA virus mutant spectrum and lethal mutagenesis events: Replicative interference and complementation by multiple point mutants. *J Mol Biol* 369(4):985–1000.
27. Rowlands DJ, Ed. (2003) Foot-and-mouth disease. *Virus Res* 91:1–161.
28. Sobrino F, Domingo E (2004) *Foot-and-Mouth Disease: Current Perspectives* (Horizon Bioscience, Wymondham, UK).
29. Mahy BWJ ed (2005) Foot-and-mouth disease virus. *Current Topics in Microbiology and Immunology*, ed Mahy BWJ (Springer, Berlin), Vol 288.
30. Mateu MG, et al. (1990) A single amino acid substitution affects multiple overlapping epitopes in the major antigenic site of foot-and-mouth disease virus of serotype C. *J Gen Virol* 71(Pt 3):629–637.
31. Arias A, et al. (2005) Mutant viral polymerase in the transition of virus to error catastrophe identifies a critical site for RNA binding. *J Mol Biol* 353(5):1021–1032.